

A Study on the Production and Emission of Marine-Derived Volatile Halocarbons

Y. Yokouchi^{1*}, A. Ooki¹, S. Hashimoto² and N. Itoh³

¹*Environmental Chemistry Division, National Institute for Environmental Studies,
16-2, Onogawa, Tsukuba, Ibaraki 305-8506, Japan*

²*Department of Chemistry, Nihon University, 3-25-40, Sakurajosui, Setagaya-ku, Tokyo 156-8550, Japan*

³*Department of Biotechnology, Toyama Prefectural University,
5180, Kurokawa, Imizu, Toyama 939-0398, Japan*

*E-mail: yokouchi@nies.go.jp

Keywords: Halocarbon; Observations; Production Mechanism; Methyl Iodide

Introduction

A considerable amount of volatile halocarbons are emitted from the ocean into the atmosphere as a result of their production from seaweeds, phytoplankton, and photolysis reactions occurring in seawater. Among these, long-lived halocarbons such as methyl chloride and methyl bromide are transported to the stratosphere, where they contribute to stratospheric ozone depletion. Organoiodine compounds, notably methyl iodide, release iodine in the marine boundary air owing to their short atmospheric lifetime. The iodine could decompose tropospheric ozone catalytically, and may contribute to new particle formation. The transport of marine-derived methyl iodide in the atmosphere is considered to be an important source of iodine to the continents. Thus, it is important to understand the sources and the emission mechanisms of marine-derived halocarbons to define the interaction between atmosphere and ocean. Here, we report extensive measurements of halocarbons in the atmosphere and the ocean, and new findings on their emission mechanism from phytoplankton

and the genetic basis of their production. This study consists of four subprojects: (1) Observations of marine-derived halocarbons in the atmosphere; (2) Ship-board observations of halocarbons in oceanic seawater; (3) Halocarbon distribution during the spring bloom in the western North Pacific; and (4) Elucidation of the mechanism of methyl halide emission from marine phytoplankton: enzymatic and genetic analyses of key enzymes catalyzing the formation of methyl iodide (CH₃I).

Methods

1. Observations of marine-derived halocarbons in the atmosphere

(1) Global distribution and seasonal concentration change of methyl iodide in the atmosphere

Methyl iodide (CH₃I) was measured as part of the National Institute for Environmental Studies (NIES) Global Halocarbon Monitoring Project, which involves periodic monitoring of atmospheric halocarbons at Alert in Canada (82.5°N, 62.5°W; semimonthly), Cape Ochiishi in Japan (43.2°N, 145.5°E; monthly), Tsukuba in Japan (36.0°N, 140.1°E, semi-

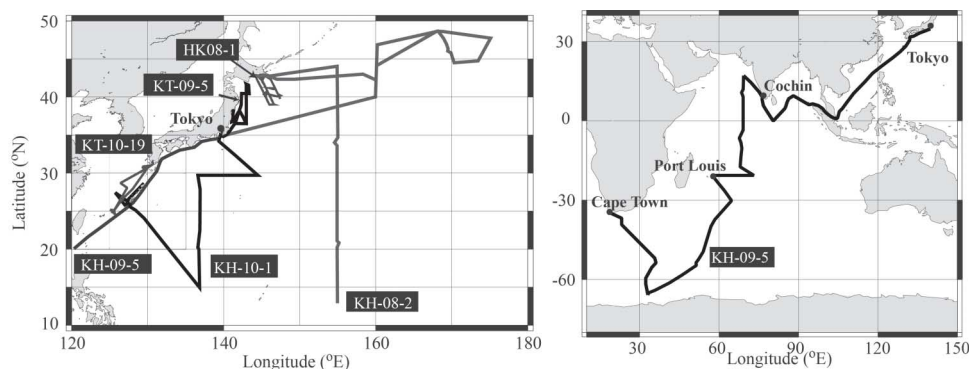


Fig. 1. Ship tracks for halocarbon monitoring.

monthly), Happo Ridge in Japan (36.7°N, 137.8°E semimonthly), Hateruma Island in Japan (24.1°N, 123.8°E; semimonthly), Cape Grim in Australia (40.4°S, 144.6°E; semimonthly), over the western Pacific Ocean (on board M/S Fuji Transworld or M/S Fuji; monthly), and over the North Pacific (on board M/S Pyxis and M/S Skaubrin; bimonthly). In 2004, year-round samples for halocarbon measurements were also obtained at San Cristobal Island (1.0°S, 89.4°W, December 2003 to December 2004) and at Syowa Station in Antarctica (68.5°S, 41.3°E, February 2004 to February 2005). To discuss the global distribution of atmospheric CH₃I, including at the latter two (equatorial and Antarctic) sites, CH₃I data covering 2004 (typically the data sets from 2003–2005) were extracted from the regular monitoring data. Among the fixed monitoring/sampling sites, Tsukuba and Happo Ridge are situated inland (approximately 50 and 40 km from the coast, respectively), whereas all the others (islands or capes) are close to the shore. All air sampling was done with stainless steel canisters. After transport to the laboratory, the samples were analyzed using a pre-concentration/capillary gas chromatograph-mass spectrometry (GC-MS). Details of the analytical procedures are described elsewhere (Li *et al.* 1994; Yokouchi *et al.* 1997).

(2) Diurnal and seasonal variations of iodocarbons in the marine atmosphere

Atmospheric CH₂I₂, CH₂I₂, CH₃I, and C₂H₅I were measured hourly with an automated preconcentration GC-MS system at ground stations on Hateruma Island and at Cape Ochiishi as a part of the NIES halocarbon monitoring project. Hateruma Island is a small island in the pathway of the Kuroshio Current in the East China Sea. It is 250 km east of Taiwan and 500 km southwest of Okinawa Island. The Cape Ochiishi monitoring station is situated on a cliff at the southern tip of Cape Ochiishi, which projects southward from the eastern coast of Hokkaido into the Oyashio Current of the western North Pacific. Details of the sampling and analytical methods have been published elsewhere (Enomoto *et al.* 2005; Yokouchi *et al.* 2006). Selected ions for quantification were *m/z* (mass to charge ratio) 268 for CH₂I₂, *m/z* 176 for CH₂I₂, *m/z* 142 for CH₃I, and *m/z* 156 for C₂H₅I. The three iodocarbons other than CH₃I were quantified on the basis of their sensitivity relative to tetrachloroethylene (C₂Cl₄) (monitored ion, *m/z* 166), which, like CH₃I, is a component of the working standard. The sensitivities relative to C₂Cl₄ were determined by the analysis of a vaporized liquid standard: A methanol solution (0.5 μL) containing a known concentration of (160–

330 ng/ μ l) of halocarbons was injected into a 5 mL glass vial whose contents were flushed with helium purge gas into the preconcentration trap. The reagents (purity >97%) were purchased from Tokyo Kasei Kogyo Co., Ltd.

2. Shipboard observations of halocarbons in oceanic seawater

(1) Shipboard observations

Halocarbon monitoring was conducted aboard the R/V *Hokko-maru* in January 2008 (cruise HK08-1), the R/V *Hakuho-maru* in July–September 2008 (cruise KH-08-2), November 2009–January 2010 (cruise KH-09-5) and May–June 2010 (cruise KH-10-5), and the R/V *Tansei-maru* in April–May 2009 (cruise KT-09-5) and September–October 2010 (cruise KT-10-19 and 21). The ship track for each cruise is shown in Fig. 1. An equilibrator/pre-concentration/gas chromatograph-mass spectrometry (GC-MS) analytical system was set up in the laboratory of each vessel.

(2) Underway measurement and GC-MS analysis

Partial pressures of halocarbons in surface seawater and air were automatically measured using an online equilibrator/pre-concentration/GC-MS system. Surface seawater was pumped from a seawater intake on the bottom of the ship (5-m depth), and supplied to the laboratory, passing through a seawater pipe with the inner wall coated with nylon for most of its length. The surface seawater was continuously supplied to a silicone membrane tube equilibrator at a flow rate of 15 L min^{-1} . Details of halocarbon measurements are described elsewhere (Ooki and Yokouchi 2008). Briefly, the equilibrator consists of six silicone tubes (length, 10 m; o.d., 2.0 mm; i.d., 1.5 mm) housed in a polyvinyl chloride pipe. Pure air was continuously supplied to the silicone tubes at a flow rate of 25 mL min^{-1} , regulating the inner pres-

sure to +0.14 MPa. Halocarbons in the liquid phase permeate the silicone membrane by dissolving into the silicone and then evaporate into the gas phase from the surface of the membrane. The gas-phase sample of halocarbons at equilibrium with the seawater could be obtained from the outlet of the silicone tube. The test for an equilibrium condition in the gas phase will be described in the next section. Outside air was drawn from the upper deck (17 m above the sea level) of the ship through a PTFE tube (length, 60 m; i.d., 11 mm) at a flow rate of 50 L min^{-1} . We obtained a portion of the air from the PTFE tube at a flow rate of 25 mL min^{-1} using a metal bellows pump. The gas phase sample (equilibrated air or outside air) was transferred to a pre-concentration/GC-MS system (Yokouchi *et al.* 2006). Partial pressures of halocarbons in the sample were measured at 70 min intervals. A gravimetrically prepared standard gas (Taiyo Nissan, Inc., Tokyo) at concentrations of 100–500 pptv for halocarbons and 10 ppbv for isoprene (C_5H_8) was quantified according to the same procedures. To calibrate the concentrations of CH_2ClI , and $\text{C}_2\text{H}_5\text{I}$, which were not contained in the standard gas, we prepared a liquid standard (methanol base) containing these compounds, along with C_2Cl_4 . We employed the relative ratios of their responses to that of C_2Cl_4 . The partial pressures of 11 halocarbons (CH_3Cl , CH_3Br , CH_3I , CH_2Cl_2 , CH_2Br_2 , CHCl_3 , CHBr_3 , CH_2ClI , $\text{C}_2\text{H}_5\text{I}$, CFC-11(CCl_3F), HCFC-22(CHClF_2)) and C_5H_8 were determined.

(3) Equilibrium condition test for halocarbons in the gas phase collected from the Silicone Membrane Tube Equilibrator

We used the following procedure to confirm that the halocarbons had equilibrated between the liquid phase and the gas phase through the membrane in the equilibrator. A water sample that had been equili-

Table 1. Henry's law constants at $T = 273.17 + 25 K (K_H^\ominus; \text{mol L}^{-1} \text{atm}^{-1})$ for halocarbons and isoprene (C_5H_8) in seawater, and their temperature dependence $d(\ln K_H)/d(1/T)$ (Ooki and Yokouchi 2011b).

VOC	This study		Previous studies		Salinity (‰)	Reference
	K_H^\ominus	$d(\ln K_H)/d(1/T)$	K_H^\ominus	$d(\ln K_H)/d(1/T)$		
CFC-11	0.0061	4900	0.0082	2700	35	Hunter-Smith <i>et al.</i> (1983)
C_5H_8	0.012	4400	0.013–0.028		0	Sander (1999)
HFC-134a	0.015	3100	0.015	3100	39.6	Zheng <i>et al.</i> (1997)
HCFC-22	0.029	3100	0.032	3000	39.6	Zheng <i>et al.</i> (1997)
CH_3I	0.14	3900	0.14	4300	30.4	Moore <i>et al.</i> (1995)
$\text{C}_2\text{H}_5\text{I}$	0.14	4800	0.14–0.18		0	Sander (1999)
CH_2Cl_2	0.36	3700	0.34	3900	34.3	Moore (2000)
CH_2ClI	0.84	6200	0.88	4300	30.4	Moore <i>et al.</i> (1995)
CH_2Br_2	0.90	4400	0.92	4400	30.4	Moore <i>et al.</i> (1995)
CHBr_3	1.0	6200	1.4	5000	30.4	Moore <i>et al.</i> (1995)

The temperature and salinity values in this study ranged from -1°C to 29.3°C and from 33.1‰ to 36.1‰, respectively.

brated with ambient air was introduced to the equilibrator, and then the partial pressures of halocarbons in the gas phase sample collected from the equilibrator ($p\text{Gas}_{\text{water}}$) were compared with those in the ambient air sample ($p\text{Gas}_{\text{air}}$), where $p\text{Gas}_{\text{water}}$ is the partial pressure of gas in water and $p\text{Gas}_{\text{air}}$ in air. If the gas phase sample from the equilibrator had reached equilibrium with the liquid phase, $p\text{Gas}_{\text{water}}$ should be the same as $p\text{Gas}_{\text{air}}$. The water equilibrated with the ambient air was continuously prepared by means of a silicone hollow fiber membrane module (NAGASEP, Nagayanagi-Kogyo Ltd.) containing 6000 silicone 20-cm tubes (o.d. 0.25 mm; i.d. 0.17 mm). We found that the variations of $p\text{Gas}_{\text{water}}$ followed those of $p\text{Gas}_{\text{air}}$ in less than an hour. This result indicates that the equilibrium of halocarbons between the liquid phase and the gas phase in the equilibrator was reached within an hour (Ooki and Yokouchi 2008).

(4) Discrete seawater sample measurement for depth profile analysis

Discrete seawater samples for depth profile analysis were collected with 12-L Niskin bottles attached to CTD observa-

tion system at sampling stations during the cruises since 2009. Seawater aliquots (124 mL) were collected in dark glass bottles, overflowing approximately 250 mL of seawater. The bottles were crimp-sealed with no headspace using a Teflon-lined septum and an aluminum cap. The sample bottles were kept in the dark at $0\text{--}4^\circ\text{C}$ until analysis, typically within 3 d. Dissolved halocarbons were collected from the seawater samples by the purge-and-trap method and transferred to the pre-concentration/GC-MS system used for the underway measurements (Ooki and Yokouchi 2011a).

(5) Determination of Henry's law constant of halocarbons in seawater

The gas partitioning between the gas phase and liquid phase is determined by its solubility, and in a dilute solution this is described as:

$$C_{\text{Gas}} = K_H \times p\text{Gas}, \quad (1)$$

where C_{Gas} is the concentration of gas (mol L^{-1}) in the liquid phase equilibrated with respect to the gas phase, $p\text{Gas}$ is the partial pressure of gas (atm) in the gas phase, and K_H is the Henry's law constant (mol

$L^{-1} \text{ atm}^{-1}$). The K_H values for dissolved gases in seawater are basic chemical constants for evaluating the gas property in the ocean. As for halocarbons in seawater, few studies have measured K_H values in seawater as a function of temperature (e.g., Moore *et al.* 1995; Moore 2000). We determined the K_H values for ten volatile organic compound species in natural seawater, including C_2H_5I and C_5H_8 the values of which are the first to be reported, by measuring the partial pressures and the molar concentrations during the cruise KH-09-5. The results are listed in Table 1.

3. Halocarbon distribution during the spring bloom in the western North Pacific

Phytoplankton is known to be a major source of halocarbons in the ocean, but there is little information about halocarbon production by phytoplankton. To investigate phytoplankton as a source of halocarbons, we analyzed the distribution of halocarbons in the air and seawater simultaneously during the spring bloom.

The concentrations of halocarbons in seawater and the mixing ratio of halocarbons in the atmosphere were measured during the spring of 2007 in the western North Pacific Ocean (37–43°N, 143–146°E), aboard the R/V *Tansei Maru* (Japan Agency for Marine-Earth Science and Technology). For the analysis of halocarbons, seawater samples were collected using 120-mL brown glass bottles. After 100 mL of water overflowed, a $HgCl_2$ solution was added (final concentration: approximately 180 mg L^{-1}) to inhibit microbial activity. The samples were immediately sealed with a hand-clipper, taking care to exclude air bubbles, and stored in the dark at 4°C until the time of analysis. The stability of halocarbons in the stored seawater samples was evaluated by analyzing the time course of halocarbon concentrations. The concentrations of halocarbons were not altered during a pe-

riod of 30 days after seawater sampling. The concentrations of gases were measured using an automated purge and trap (AQUA PT 5000J Plus; GL-Science, Tokyo, Japan) gas chromatograph-mass spectrometer (GC-MS, Agilent 6890-5973; Agilent Technologies, Tokyo, Japan) within one month. Briefly, each sample was purged with ultrapure helium, and the dissolved volatile compounds were pre-concentrated in a trap column (Aqua trap 2, GL-Science) that was maintained at room temperature. Compounds were released from the trap column by heating to 260°C, and the gases were introduced into the capillary column (DB-624, length, 20 m; i.d., 0.18 mm; and film thickness, 1 μm ; Agilent Technologies, Tokyo, Japan) after cryo-focusing. Halocarbons were quantified according to the retention times and peak area of the calibration standards. Outside air in the marine boundary layer was drawn from the upper deck of the ship (8 m above the sea level), and transferred to a pre-concentration/capillary GC-MS system. Details of the sampling and analytical methods have been reported elsewhere (Yokouchi *et al.* 2006). Selected ion monitoring was employed and the ions monitored for quantification were mass to charge ratio (m/z) 50 for CH_3Cl , m/z 94 for CH_3Br , m/z 176 for CH_2ClI , and m/z 268 for CH_2I_2 . A gravimetrically-prepared standard gas containing CH_3Cl (500 ppt), CH_3Br (100 ppt) and tetrachloroethylene C_2Cl_4 (100 ppt) (Taiyo Nippon Sanso Corporation) was analyzed for quantification at least once a day. To calibrate the concentrations of CH_2ClI and CH_2I_2 , which were not contained in the standard gas, a liquid standard containing these compounds along with C_2Cl_4 was prepared before and after the cruise. We employed the relative ratios of CH_2ClI and CH_2I_2 responses to that of C_2Cl_4 to calculate the concentrations of CH_2ClI and CH_2I_2 in the atmosphere.

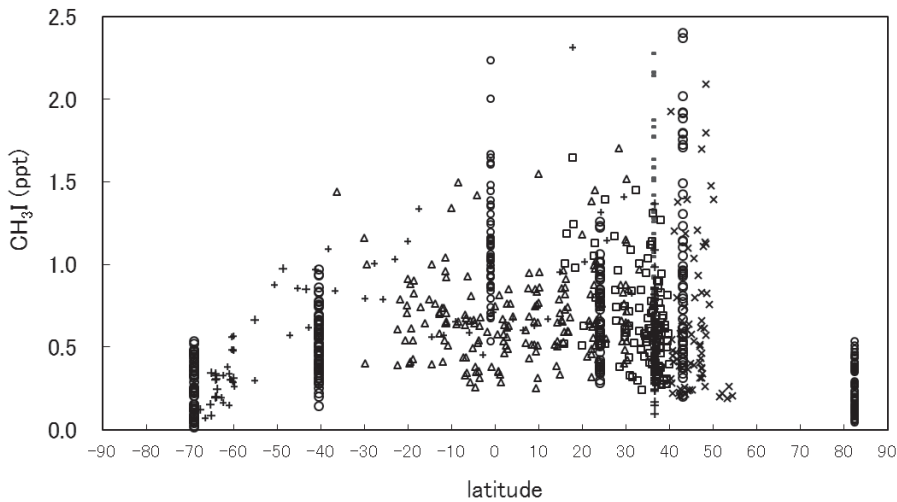
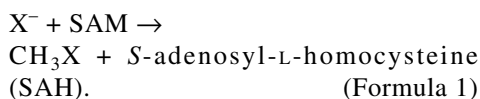


Fig. 2. Latitudinal variation of atmospheric CH_3I (2003–2005) (modified from Yokouchi et al. (2008)).

4. Elucidation of the mechanism of methyl halide emission from marine phytoplankton: enzymatic and genetic analyses of key enzymes catalyzing the formation of CH_3I

It is known that marine phytoplankton and macroalgae have the ability to transform oceanic iodide ions (I^-) into alkyl halide compounds, such as CH_3I , and to emit them into the marine environment. Chloride methyltransferase (*S*-adenosyl-*L*-methionine: halide ion methyltransferase, HMT) that catalyzes the formation of methyl halides via *S*-adenosyl-*L*-methionine (SAM) as a methyl donor, was isolated from the red marine algae *Endocladia muricata*, and the methylation mechanism was determined as follows (Wuosmaa and Hager 1990):



Homologues of this enzyme have been found in several organisms, such as higher

plants (Attieh et al. 2000; Itoh et al. 2009), algae (Itoh et al. 1997), fungi, and soil bacteria (Amachi et al. 2001), and some of these homologues have been characterized in detail. Data shows that they also catalyze the methylation of thiol substrates, such as the bisulfide ion ($[\text{SH}]^-$) and the thiocyanate ion ($[\text{SCN}]^-$), to give CH_3SH or CH_3SCN , respectively.

In this study, various marine phytoplankton were cultivated in order to clarify the molecular formation mechanism of methyl halides and to establish a correlation between intracellular halide ion methyl transferase/halide ion thiol methyl transferase (HTM/HTMT) activity and CH_3X emission. The enzyme genes were isolated from marine phytoplankton, verified, expressed in *E. coli*, and characterized in detail. The results clarify the mechanism of the biogenic emission of methyl halides in oceans.

Experimental details for strains, cultivation of phytoplankton, analytical conditions of GC-MS, enzyme assay, preparation of genomic DNA, plasmid construc-

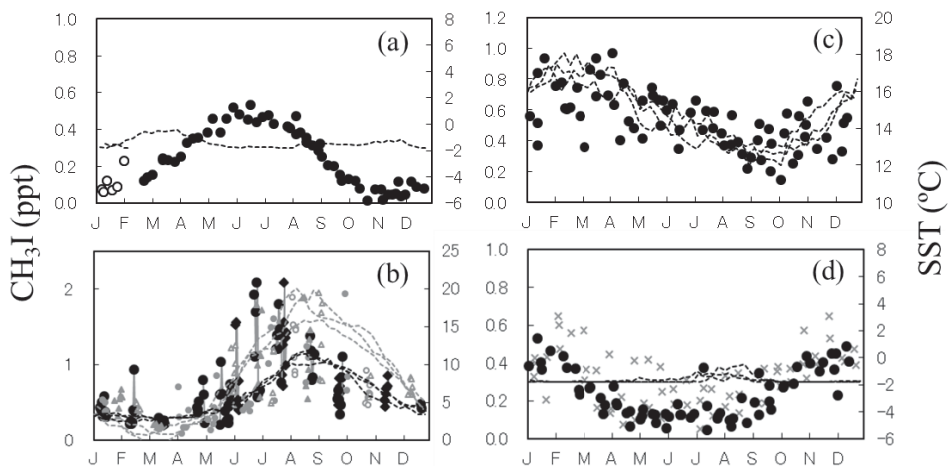


Fig. 3. Seasonal variation of atmospheric CH₃I observed at (a) Alert (2003–2005), (b) North Pacific Ocean (2003–2005), (c) Cape Grim (2003–2005), (d) Syowa Station in Antarctica (February 2004 to February 2005) (modified from Yokouchi *et al.* (2008)).

tion, and expression and purification of recombinant enzymes are described in Itoh *et al.* (2009) and Toda and Itoh (2010).

Results and Discussions

1. Observations of marine-derived halocarbons in the atmosphere

(1) Global Distribution and Seasonal Concentration Change of Methyl Iodide in the Atmosphere

Latitudinal distribution

The observed CH₃I mixing ratios ranged from 0.01 ppt to 5.5 ppt. All data were plotted against latitude (Fig. 2), and the mixing ratios tended to be higher at low to mid-latitudes. Median values for the fixed coastal observation sites were 0.20 ppt at Alert, 0.72 ppt at Cape Ochiishi, 0.77 ppt at Hateruma Island, 1.05 ppt at San Cristobal Island, 0.52 ppt at Cape Grim, and 0.23 ppt at Syowa Station, suggesting increasing concentrations from high to low latitudes. However, CH₃I mixing ratios measured over the tropical western Pacific

were around 0.6 ppt—close to, or lower than, those from mid-latitudes. We also examined the data by dividing them according to 10° intervals of latitude, and found that CH₃I mixing ratios within 10° of the equator were lower than those from further north (10–20°N) or south (10–20°S) by approximately 15%.

The high levels of CH₃I observed at San Cristobal Island might be related to high biological productivity in the eastern Pacific or in the surrounding coastal waters. On the other hand, the low concentrations of CH₃I over the tropical western Pacific might be attributable to low bioproductivity in that region. Rapid atmospheric dilution resulting from active convection might be responsible, to some extent, for the slight drop in CH₃I concentrations observed at the equator over the western Pacific.

The atmospheric CH₃I levels presented here are generally consistent with cruise data (Atlantic, Pacific, and Southern Ocean) recently reported by Butler *et al.* (2007).

Seasonal variation

Seasonal trends of atmospheric CH₃I showed quite different patterns at different latitudes, although no systematic seasonal change was found at the equator. The seasonal variations from Syowa, Northern Pacific, Cape Grim and Alert are shown in Fig. 3 as examples. The CH₃I concentrations observed at mid-latitudes, over the North Pacific, at Cape Ochiishi, and at Cape Grim, were higher in summer and early autumn than in other seasons of the year. A less-pronounced change in the CH₃I concentration was observed at Hateruma Island, which is at a lower latitude (24.1°N). The most-striking seasonal variations were observed in the Arctic (Alert) and in Antarctica (Syowa Station). At these high-latitude sites, CH₃I was detected at low mixing ratios, ranging from <0.02 to 0.5 ppt, and its seasonal variation showed a sinusoidal curve with a winter maximum, which was clearly inversely correlated with that of the expected incident solar radiation (highest in June and lowest in December in the Northern Hemisphere, and vice versa in the Southern Hemisphere). A possible explanation for this is that CH₃I emission from the surrounding cold oceans is very small throughout the year, and long-range transported CH₃I from mid-latitudes is more responsible for the atmospheric CH₃I in the polar regions. In summer, intense solar radiation could enhance photolytic decomposition of atmospheric CH₃I during long-range transport, while, during the dark winter months, more CH₃I would be transported from mid-latitudes without loss due to photolysis. Thus, the intensity of solar radiation in high-latitudes could account for the seasonal change of atmospheric CH₃I observed there.

The seasonal variations suggested a positive correlation between atmospheric CH₃I and SST at all mid-latitude marine sites (North Pacific, Cape Ochiishi, and Cape Grim) and at Hateruma Island. The

correlation coefficients (R^2) between the atmospheric CH₃I mixing ratio and SST were 0.52 for the North Pacific-A, 0.49 for Cape Ochiishi, 0.41 for Cape Grim, 0.40 for the North Pacific and 0.19 for Hateruma Island, while the data from San Cristobal Island as well as from both polar sites showed no correlation. High correlation between atmospheric CH₃I and SST at mid-latitudes had also been found in previous work, where the finding was explained by the photochemical production of CH₃I rather than biogenic emission (Yokouchi *et al.* 2001). The main reason was that a higher emission of CH₃I from warmer seawater was well reflected in its atmospheric concentration, in spite of the fact that CH₃I is easily decomposed by photolysis in the atmosphere (atmospheric lifetime, 2–5 days (Zafiriou 1975; Rattigan *et al.* 1997)). It is very likely that photochemical production of CH₃I in the water was compensating for its photolytic decay in the atmosphere, leading to the lack of a prominent effect of solar radiation on the atmospheric CH₃I concentration.

At the two inland stations, the mean mixing ratio of CH₃I was 0.87 ppt (Tsukuba) and 0.46 ppt (Happo Ridge): in particular, the spring/summer CH₃I mixing ratios at Tsukuba (up to 4 ppt) exceeded the values at oceanic sites. These values might reflect terrestrial sources, such as rice fields, in addition to the transport from oceanic sources. Terrestrial sources might also contribute to the CH₃I mixing ratios observed at Cape Ochiishi, because the site is occasionally affected by inland air masses.

(2) Diurnal and seasonal variations of iodocarbons in the marine atmosphere

During the period between August 2008 and January 2010, more than 9000 and 7000 data sets of the four targeted iodocarbons in the atmosphere were obtained at Hateruma Island and Cape Ochiishi, respectively. These are the first

full-year high-frequency data sets for all these compounds. Among them, the data for 15 September to 28 October, 2009, from Hateruma Island and Cape Ochiishi are shown in detail in Fig. 4.

Different patterns of seasonal and diurnal variations were apparent between two groups: CH_2ClI and CH_2I_2 , and CH_3I and $\text{C}_2\text{H}_5\text{I}$. It is likely that different production and removal processes control the concentrations of the compounds in each group. Therefore, we grouped the iodocarbons into two categories, (1) CH_2ClI and CH_2I_2 , and (2) CH_3I and $\text{C}_2\text{H}_5\text{I}$, to examine the variations in their concentrations.

Atmospheric concentrations of CH_2ClI and CH_2I_2 at Hateruma Island and Cape Ochiishi

The mean mixing ratios of CH_2ClI were 0.12 pptv at Hateruma Island and 0.18 pptv at Cape Ochiishi, which are within the range of previously reported values. However, the mean mixing ratios of CH_2I_2 —0.008 pptv at Hateruma Island and 0.03 pptv at Cape Ochiishi—are at the low end of previously reported data. The mixing ratios of both CH_2ClI and CH_2I_2 showed high temporal variability, much higher at night than in the daytime, and CH_2I_2 , in particular, was rarely detected at midday. This finding can be explained by their short atmospheric lifetimes (several hours for CH_2ClI and several minutes for CH_2I_2) during the day due to photolysis (e.g., Rattigan *et al.* 1997; Mössinger *et al.* 1998). Seasonal variations of the CH_2ClI and CH_2I_2 mixing ratios differed considerably between Cape Ochiishi and Hateruma Island. At Cape Ochiishi, both compounds were much more abundant in summer/autumn than in winter/spring, and their concentrations were well correlated. Considering that macroalgae are abundant in the marine waters surrounding Cape Ochiishi, and algal blooms develop in summer and autumn, algae are likely to be the

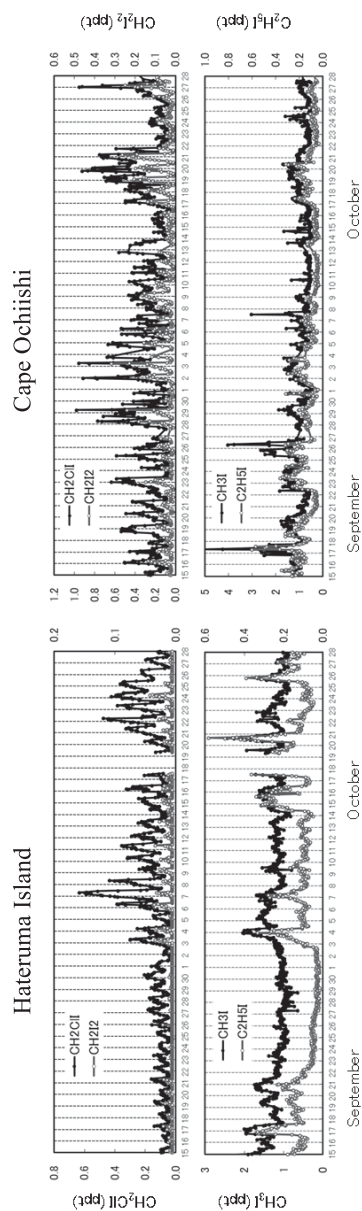


Fig. 4. Variations of the mixing ratios of the iodocarbons measured at Hateruma Island (left) and Cape Ochiishi (right) between 15 September and 28 October, 2009. From the top, CH_2ClI (black) and CH_2I_2 (grey), and CH_3I (black) and $\text{C}_2\text{H}_5\text{I}$ (grey) (modified from Yokouchi *et al.* (2011)).

main source of CH_2ClI and CH_2I_2 there. At Hateruma Island, in contrast, the CH_2ClI and CH_2I_2 mixing ratios were highest in autumn and lowest in summer. The absence of a summer increase of CH_2ClI at Hateruma Island is consistent with a low bioactivity in the surrounding ocean, and the photochemical production of marine dissolved organic matter and dissolved iodide might be an important source of CH_2ClI there.

An outstanding feature of the CH_2ClI mixing ratio in the atmosphere at Hateruma Island, other than the diurnal variation related to solar radiation, was its close correlation with wind speed (e.g., $R^2 = 0.58$ for autumn nighttime data). Considering that the air-sea exchange coefficient (K_w) is approximately proportional to the square of the wind speed (e.g., Wanninkhof 1992), a significant correlation between the atmospheric mixing ratio and wind speed suggests that the sea-to-air flux is well reflected in the atmospheric mixing ratio, and also that the air-sea concentration difference is fairly constant throughout the observation period.

We estimated the CH_2ClI flux in the Hateruma Island area by two methods, both based on a simple box model: (1) 28–20 $\text{ng m}^{-2} \text{h}^{-1}$, or 3.8–2.7 $\text{nmol m}^{-2} \text{day}^{-1}$ from the average accumulation rate of atmospheric CH_2ClI in the nighttime (19:00 to 02:00 LT), and (2) 30–100 $\text{ng m}^{-2} \text{h}^{-1}$ (4–13 $\text{nmol m}^{-2} \text{day}^{-1}$) from the photolysis rate in the daytime. Likewise, the flux of CH_2I_2 was preliminarily calculated to be $\sim 14 \text{ ng m}^{-2} \text{ h}^{-1}$ (1.3 $\text{nmol m}^{-2} \text{ day}^{-1}$).

Atmospheric concentrations of CH_3I and $\text{C}_2\text{H}_5\text{I}$ at Hateruma Island and Cape Ochiishi

The mean mixing ratio of CH_3I at Hateruma Island and Cape Ochiishi were 1.2 pptv and 0.81 pptv, respectively, which are in the range of typical background mixing ratios of CH_3I (0.2–2 pptv) (Yokouchi

et al. 2008). There are fewer measurements reported for $\text{C}_2\text{H}_5\text{I}$ than CH_3I . The mean mixing ratios of $\text{C}_2\text{H}_5\text{I}$, 0.15 pptv at Hateruma Island and 0.08 pptv at Cape Ochiishi, are close to those from Asian seas, <0.03 to 0.31 pptv (Yokouchi *et al.* 1997). CH_3I and $\text{C}_2\text{H}_5\text{I}$ measured at Hateruma Island and Cape Ochiishi showed little diurnal variation, in contrast to the remarkable diurnal variation of CH_2ClI and CH_2I_2 described above. Short-term variations of CH_3I and $\text{C}_2\text{H}_5\text{I}$ were very similar with each other at both Hateruma Island and Cape Ochiishi, strongly suggesting that they have common sources and sinks. Because CH_3I is probably produced in the open ocean by a light-dependent production pathway that is not directly dependent on biological activity (Yokouchi *et al.* 2001; Richter and Wallace 2004), the observed high correlation between CH_3I and $\text{C}_2\text{H}_5\text{I}$ suggests that similar non-biogenic emissions are important $\text{C}_2\text{H}_5\text{I}$ sources. A remarkable feature of the variations of CH_3I and $\text{C}_2\text{H}_5\text{I}$ was the repeated sharp increases followed by gentle declines on a timescale of hours ~ days in winter and spring, when the island is affected by the outflow of atmospheric pollutants from the southern Asian continent. Comparison of the variations of CH_3I and $\text{C}_2\text{H}_5\text{I}$ with those of a typical anthropogenic compound, HCFC-22 (difluorochloromethane) suggested the possibility that the two iodocarbon compounds have anthropogenic sources in the Asian continent.

2. Shipboard observations of halocarbons in oceanic seawater

(1) Partial pressures and sea-to-air fluxes of mono-halomethanes in the NW Pacific Ocean

The partial pressures and saturation anomalies of mono-halomethanes (CH_3Cl , CH_3Br , CH_3I) in the surface seawater of the subarctic and subtropical NW Pacific Oceans are discussed taking the observa-

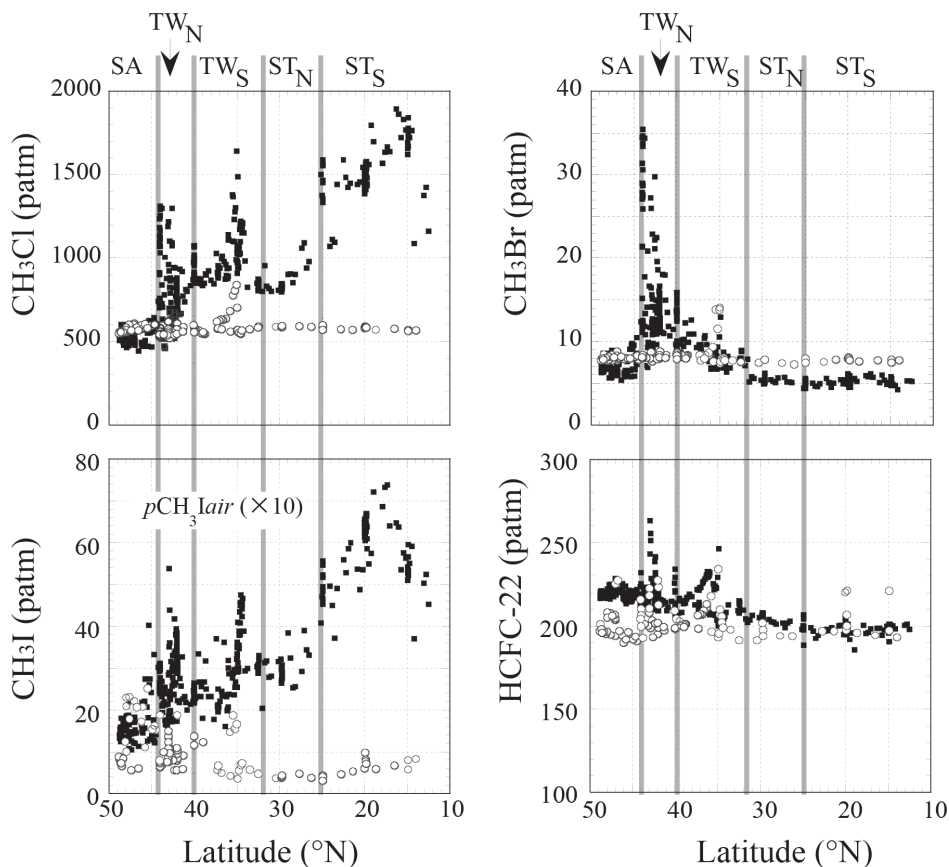


Fig. 5. Latitudinal distributions of partial pressures (patm) in surface seawater (■) and air (○). Water types (SA, MW_N , MW_S , and ST_N and ST_S) are separated by gray lines (Ooki *et al.* 2010).

tion results of KH-08-2 in the period July–September 2008. From the conductivity-temperature-depth (CTD) profiles obtained at intervals of 1° along 155°E from 44°N to 12°N , we classified the surface seawater into 5 water types: (1) Subarctic water (SA) in $44\text{--}49^\circ\text{N}$ (approximately $\text{SST} = 11\text{--}16^\circ\text{C}$); (2) Northern mixed water (MW_N) in $40\text{--}44^\circ\text{N}$ (approximately $\text{SST} = 16\text{--}20^\circ\text{C}$); (3) Southern mixed water (MW_S) in $32\text{--}40^\circ\text{N}$ (approximately $\text{SST} = 20\text{--}27^\circ\text{C}$); (4) Northern subtropical water (ST_N) in $32\text{--}25^\circ\text{N}$ (approximately $\text{SST} = 27\text{--}28^\circ\text{C}$); (5) Southern subtropical water (ST_S) in $25\text{--}12^\circ\text{N}$ (approximately $\text{SST} = 28\text{--}30^\circ\text{C}$). Details of water mass classi-

cation are described in Ooki *et al.* (2010). The latitudinal distributions of $p\text{Gas}_{\text{water}}$ and $p\text{Gas}_{\text{air}}$ are shown in Fig. 5, and those averages and ranges are listed in Table 2. The saturation anomaly of a Gas (S_{Gas}) is defined as:

$$S_{\text{Gas}} = (p\text{Gas}_{\text{water}} - p\text{Gas}_{\text{air}})/p\text{Gas}_{\text{air}} \quad (2)$$

The $p\text{HCFC-22}_{\text{water}}$ in SA, MW_N , MW_S , and ST_N waters were slightly higher than the average $p\text{HCFC-22}_{\text{air}}$ of all the samples, whereas $p\text{HCFC-22}_{\text{water}}$ in ST_S water was slightly below the average of $p\text{HCFC-22}_{\text{air}}$. We found a higher $S_{\text{HCFC-22}}$ in the colder waters, ranging from -0.02

Table 2. Ranges (averages) of $p\text{Gas}_{\text{air}}$ and $p\text{Gas}_{\text{water}}$ (patm) in different water types (Ooki *et al.* 2010).

	CH_3Cl		CH_3Br		CH_3I		HCFC-22	
	Water	Air	Water	Air	Water	Air	Water	Air
SA	446–742 (537)	549–607 (579)	5.4–12 (7.1)	7.7–8.9 (8.1)	11–40 (17)	0.56–2.5 (1.5)	214–229 (220)	190–228 (200)
MW _N	462–1313 (841)	521–609 (559)	7.0–35 (16)	7.6–8.8 (8.2)	16–54 (27)	0.56–1.9 (0.91)	209–263 (220)	193–228 (204)
MW _S	801–1645 (1007)	546–840 (603)	6.4–13 (8.4)	7.4–14 (8.7)	16–48 (30)	0.35–1.9 (0.84)	200–246 (212)	192–234 (204)
ST _N	798–1095 (871)	583–597 (590)	4.9–7.9 (5.5)	7.3–7.9 (7.6)	25–39 (30)	0.36–0.48 (0.41)	199–208 (204)	192–202 (196)
ST _S	1072–1893 (1530)	564–600 (578)	4.3–6.2 (5.2)	7.5–8.1 (7.8)	37–74 (58)	0.30–0.98 (0.63)	186–207 (199)	194–221 (204)
All	446–1894 (959)	521–840 (583)	4.3–35 (9.8)	7.3–14 (8.2)	11–74 (32)	0.30–2.5 (0.99)	186–263 (214)	190–234 (203)

to 0.10. As for the inert gas of HCFC-22, the $S_{\text{HCFC-22}}$ values from +0.10 (SA) to +0.04 (MW_S) can be explained by the rapid decrease of solubility as a result of the rise in SST. In contrast to HCFC-22, the partial pressures of 3 mono-halomethanes in the surface seawater varied greatly among water regions. On the whole, $p\text{CH}_3\text{Cl}_{\text{water}}$ increased toward the south, and the latitudinal distribution of $p\text{CH}_3\text{Cl}_{\text{water}}$ had a maximum, both in the MW_N and ST_S waters. For most of the SA water, $p\text{CH}_3\text{Cl}_{\text{water}}$ was less than $p\text{CH}_3\text{Cl}_{\text{air}}$, with an average $S_{\text{CH}_3\text{Cl}}$ of -0.07 . In MW_N water which had a high biological productivity, high levels of $p\text{CH}_3\text{Cl}_{\text{water}}$ (up to 1313 patm) were frequently observed. The highest $p\text{CH}_3\text{Cl}_{\text{water}}$ in ST_S (1893 patm) was 1.6 times the previously reported highest value (1200 patm) in the subtropical East Pacific (Moore *et al.* 1996). As for CH_3Br , the latitudinal distribution of $p\text{CH}_3\text{Br}_{\text{water}}$ had an obvious maximum in MW_N water. In SA water, most $p\text{CH}_3\text{Br}_{\text{water}}$ values were less than $p\text{CH}_3\text{Br}_{\text{air}}$, with $S_{\text{CH}_3\text{Br}} = -0.12$, and in MW_N water, high levels of $p\text{CH}_3\text{Br}_{\text{water}}$ (up to 35 patm) were frequently present, with $S_{\text{CH}_3\text{Br}} = 0.95$. In ST_N and ST_S waters, $p\text{CH}_3\text{Br}_{\text{water}}$ remained below $p\text{CH}_3\text{Br}_{\text{air}}$ with average $S_{\text{CH}_3\text{Br}}$ values of -0.27 and -0.33 , respectively. The low values of

$S_{\text{CH}_3\text{Br}}$ in SA, ST_N and ST_S (-0.12 , -0.27 and -0.33) were similar to those in the polar and tropical waters of the Atlantic and Pacific Oceans ($S_{\text{CH}_3\text{Br}} = -0.15$ to -0.36) (King *et al.* 2002). $S_{\text{CH}_3\text{Br}}$ of 0.95 in MW_N was higher than the supersaturation ($S_{\text{CH}_3\text{Br}} = 0.5$ – 0.6) observed in Atlantic Ocean water (41 – 42°N) in the summer of 1998 (King *et al.* 2000). As with CH_3Cl , $p\text{CH}_3\text{I}_{\text{water}}$ increased toward the south, and the latitudinal distribution of $p\text{CH}_3\text{I}_{\text{water}}$ had a maximum both in the MW_N and ST_S waters. During the cruise, $p\text{CH}_3\text{I}_{\text{water}}$ was much higher than $p\text{CH}_3\text{I}_{\text{air}}$ with an average $S_{\text{CH}_3\text{I}}$ of 31. High levels of $p\text{CH}_3\text{I}_{\text{water}}$ (up to 54 patm) were frequently observed in MW_N water. The $p\text{CH}_3\text{I}_{\text{water}}$ in ST_S of NW Pacific (average 58 patm; range 38–74 patm) was somewhat higher than the previously reported values for tropical water (average 25 patm, range 11–44 patm), central gyre water (average 21 patm, range 6.2–49 patm), and coastal water (average 15 patm, range 2.9–32 patm) of the Atlantic and E Pacific Oceans observed during various seasons (Butler *et al.* 2007).

The higher (or lower) saturation anomalies of mono-halomethanes compared to those of HCFC-22 indicate a net production (or loss) of individual mono-

Table 3. Averages of sea-to-air flux of 3 mono-halomethanes, wind speed (WS) and sea surface temperature (SST) (Ooki *et al.* 2010).

	WS	SST	CH ₃ Cl	CH ₃ Br	CH ₃ I
	m s ⁻¹	°C	nmol m ⁻² h ⁻¹		
SA	4.1	13.9	-0.71	-0.03	+0.15
MW _N	5.2	17.8	+4.1	+0.20	+0.37
MW _S	5.7	25.3	+4.2	+0.02	+0.39
ST _N	6.1	27.4	+4.1	-0.05	+0.51
ST _S	4.4	29.3	+5.5	-0.03	+0.41
All	5.1	24.6	+4.2	-0.02	+0.39

halomethanes in seawater. From the saturation anomaly results and the observed meteorological data, the sea-to-air fluxes of 3 mono-halomethanes were calculated from Eq. (3), and the average fluxes are listed in Table 3.

$$\begin{aligned} & \text{Sea-to-air flux} \\ & = K \cdot (p\text{Gas}_{\text{water}} - p\text{Gas}_{\text{air}}) \cdot K_{\text{H}} \quad (3) \end{aligned}$$

where K is the gas transfer velocity (cm s⁻¹), which depends on wind speed (Wanninkhof 1992). K_{H} is the temperature-dependent Henry's law constant (mol L⁻¹ atm⁻¹) obtained from Moore (2000) for CH₃Cl, Wilhelm *et al.* (1977) for CH₃Br, and Table 1 for CH₃I.

The MW_N water with a high biological productivity had high sea-to-air fluxes of 3 mono-halomethanes, apparently due to the phytoplankton production of halocarbons. The oligotrophic subtropical water with high SST had the highest fluxes of CH₃Cl and CH₃I among all water types. We concluded that the summertime subtropical NW Pacific is an important source of CH₃Cl and CH₃I (Ooki *et al.* 2010). We proposed the following hypotheses for explaining the aspects of mono-halomethane distributions in the subtropical and subarctic NW Pacific: (1) photochemical productions of CH₃I and CH₃Cl largely contributed to their enrichment in the surface of subtropical water, which has a

strong light intensity and high SST above 28°C; (2) dominant phytoplankton species in the subtropical water such as *Prochlorococcus*, emitted large amounts of CH₃I and CH₃Cl; and (3) the bacterial decomposition of CH₃Cl prevailed its phytoplankton production in the subarctic water, and bacterial decomposition of CH₃Br prevailed both in the subarctic and subtropical waters. These presumed production/decomposition processes would depend on the sea water temperature.

(2) Source analysis of dichloromethane (CH₂Cl₂) in the North and South Indian Oceans

We analyzed the sources of CH₂Cl₂ in seawater from the observation results of KH-09-5 in the North and South Indian Oceans. The latitudinal distribution of $p\text{CH}_2\text{Cl}_2_{\text{air}}$ and $p\text{CH}_2\text{Cl}_2_{\text{water}}$ from the North Indian Ocean to the Southern Ocean are shown in Fig. 6. An expanded view of the partial pressures in the Southern Hemisphere is shown in the right-hand panel. High values for $p\text{CH}_2\text{Cl}_2_{\text{air}}$ (100 patm, average) and $p\text{CH}_2\text{Cl}_2_{\text{water}}$ (76 patm, average) were found in the North Indian Ocean due to the terrestrial air outflow from India. Both air and water partial pressures dropped steeply southward to below 20 patm at 10°S, where the southern boundary of the Inter Tropical Convergence Zone (ITCZ) is found. In the South Indian and Southern Oceans between 10°S and 65°S, the observed average $p\text{CH}_2\text{Cl}_2_{\text{air}}$ of 11.5 patm is in good agreement with the recent value of the marine background air level measured at Cape Grim (NOAA, CMDL Report 27). Between 10°S and 40°S, most $p\text{CH}_2\text{Cl}_2_{\text{water}}$ values were higher than $p\text{CH}_2\text{Cl}_2_{\text{air}}$ with an $S_{\text{CH}_2\text{Cl}_2}$ of +0.1 – +0.2. The $S_{\text{CH}_2\text{Cl}_2}$ values were higher than the average $S_{\text{CFC-11}}$ of +0.04 caused by a decrease in solubility as a result of a summertime SST rise. Such high levels of $S_{\text{CH}_2\text{Cl}_2}$ compared to $S_{\text{CFC-11}}$ indicates the production of CH₂Cl₂ in seawater.

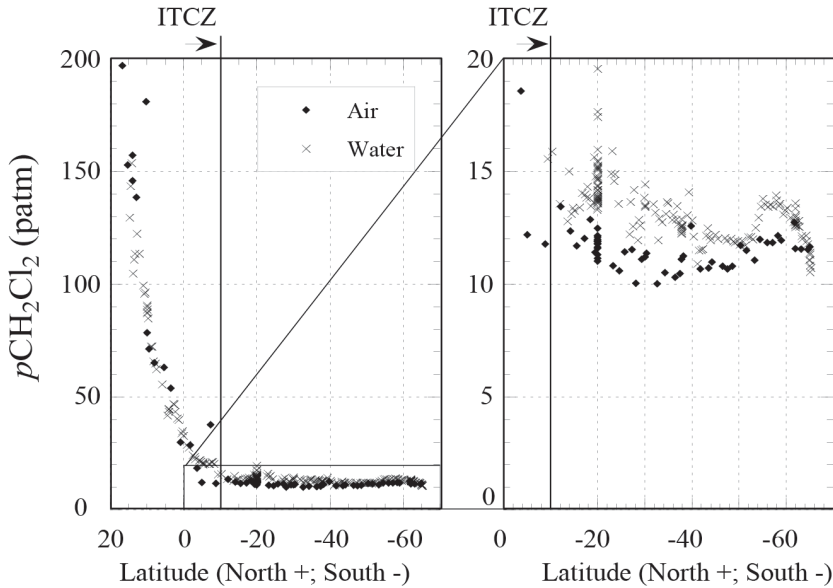


Fig. 6. Latitudinal distributions of partial pressures (patm) of CH_2Cl_2 in air (\blacklozenge) and surface seawater (\times) (Ooki and Yokouchi 2011a).

To assess the excess $S_{\text{CH}_2\text{Cl}_2}$ (>0) caused by oceanic production, we estimated the effects that change the $S_{\text{CH}_2\text{Cl}_2}$ value. The CH_2Cl_2 saturation anomaly in the Southern Hemisphere is mainly affected by three types of processes. First are the physical processes, such as SST change and water mixing, which are evident in the behavior of $\text{SA}_{\text{CFC-11}}$. Next are the seasonal changes in $p\text{CH}_2\text{Cl}_{2\text{air}}$, with late-summer minima and late-winter maxima. Third are the processes involved with the in-situ production of CH_2Cl_2 in seawater. We will account for the effect of the summertime decline of $p\text{CH}_2\text{Cl}_{2\text{air}}$ on the $\text{SA}_{\text{CH}_2\text{Cl}_2}$ increase. From November to December, $p\text{CH}_2\text{Cl}_{2\text{air}}$ at Cape Grim, Tasmania (41°S) decreased by approximately 0.5 patm over 2 weeks (Simmonds *et al.* 2006). Such a decrease would raise $\text{SA}_{\text{CH}_2\text{Cl}_2}$ to approximately 0.06. In contrast, AGAGE reported no significant seasonal change of $p\text{CH}_2\text{Cl}_{2\text{air}}$ in the low-latitude region of American Samoa (14°S). Therefore, we use the excess values of 0 and 0.06 as the

portion of $S_{\text{CH}_2\text{Cl}_2}$ attributable to seasonal effects. We estimated the excess $S_{\text{CH}_2\text{Cl}_2}$ ($\Delta S_{\text{CH}_2\text{Cl}_2}$) after subtracting the effects of the summertime sea-surface temperature increase and the summertime decrease of the atmospheric CH_2Cl_2 level, i.e., the $\Delta S_{\text{CH}_2\text{Cl}_2}$ value means the supersaturation caused by in-situ production of CH_2Cl_2 in seawater. The average sea-to-air flux of CH_2Cl_2 produced in seawater between $10^\circ\text{--}40^\circ\text{S}$ was calculated to be $0.29\text{--}0.43 \mu\text{g m}^{-2} \text{d}^{-1}$.

To discuss the sources of CH_2Cl_2 in seawater, vertical profiles of CH_2Cl_2 concentrations in the North Indian Ocean (10°N) and South Indian Ocean (20°S) are shown in Fig. 7 together with chlorophyll-*a* and temperature profiles. The chlorophyll-*a* concentration maximum in each profile was in the subsurface layer below the mixed-layer depth (MLD). In the North Indian Ocean, the CH_2Cl_2 concentration maximum was found near the surface, resulting from the oceanic uptake of anthropogenic CH_2Cl_2 from the air. In contrast,

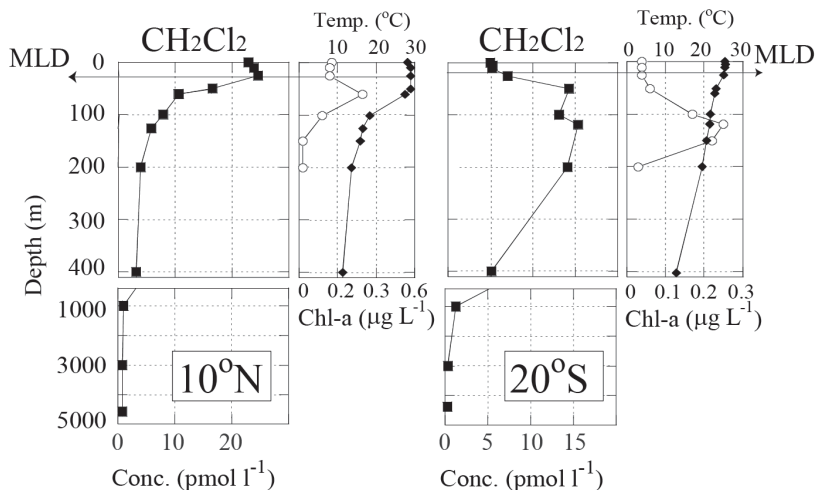


Fig. 7. Vertical distributions of CH_2Cl_2 (■), chlorophyll-*a* (○) and seawater temperature (◆) in the North Indian Ocean (10°N) and the South Indian Ocean (20°S) (Ooki and Yokouchi 2011a).

in the South Indian Ocean, the concentration maximum was in the subsurface layer (20–150 m) as was the concentration maximum of chlorophyll-*a*. We conclude that phytoplankton production of CH_2Cl_2 led to the concentration maximum in the subsurface layer, and resulted in the high saturation anomaly ($S_{\text{CH}_2\text{Cl}_2} = +0.1 \sim +0.2$) and the sea-to-air flux ($0.29\text{--}0.43 \mu\text{g m}^{-2} \text{d}^{-1}$) in the South Indian Ocean ($10^\circ\text{--}40^\circ\text{S}$) (Ooki and Yokouchi 2011a).

3. Halocarbon distribution during spring bloom in the western North Pacific

(1) Hydrographic conditions

In the temperature-salinity scatter diagram analyses, the sampling stations were divided into water regions including the Oyashio region (Stns. A1, A2, B1, B2, and C), Tsugaru warm current region (Stns. D1 and D2), Kuroshio region (Stns. E1 and E2), and the cold lower-layer water region. This water region discrimination is based on the definition: “all waters occupying some specific region on the temperature-salinity plane” (Hanawa and Mitsudera 1987). The coexistence of the Tsugaru Warm Current (sea water temperature >

5°C , salinity 33.7–34.2, density (σ_t) < 24.0), the Oyashio (sea water temperature < 7°C , salinity 33.0–33.7, σ_t > 26.7), and the Kuroshio (salinity 34.2–35.0, σ_t 26.7–24.0) regions, result in a wide variety of temperature-salinity combinations in the seawater (Hanawa and Mitsudera 1987).

(2) Relationship between halocarbons and chlorophyll-*a*

The depth-averaged concentrations of chlorophyll-*a* (Chl.-*a*) in the water column at each station were from 0.28 to 2.08 $\mu\text{g L}^{-1}$ for the Oyashio region, 0.46 to 0.48 $\mu\text{g L}^{-1}$ for the Tsugaru warm current region, and 0.65 to 0.75 $\mu\text{g L}^{-1}$ for the Kuroshio region. High concentrations of Chl.-*a* were observed in the Oyashio region. However, no apparent Chl.-*a* increase was observed in the vertical profiles of Chl.-*a* from the Tsugaru warm current and Kuroshio regions. Vertical profiles of the CH_3Cl , CH_3Br , CH_2I_2 , and CH_2ClI concentrations indicate that higher concentrations of CH_3Br , CH_2I_2 , and CH_2ClI were detected in the Tsugaru warm current region. The maximum concentrations of CH_2I_2 and CH_2ClI were observed at ap-

proximately 10–30-m and 5–20-m depths, respectively. These results are consistent with the findings of a study carried out by Moore and Tokarczyk (1993), in which the maximum concentration of CH_2ClI was observed at the surface at a site in the North Atlantic where the concentration of CH_2I_2 peaked at approximately 50-m depth. Yamamoto *et al.* (2001) also reported a similar depth profile, where the maximum concentrations of CH_2I_2 were found between 50–70 m and those of CH_2ClI were found near or above the maximum CH_2I_2 depth. These results indicate that CH_2I_2 and CH_2ClI production occurred in the euphotic zone and suggest that the production of CH_2ClI was derived at least in part from CH_2I_2 by a photochemical reaction. The results of a correlation study revealed a significant positive correlation between the concentrations of CH_2ClI and CH_2I_2 in seawater ($r^2 = 0.810$, $n = 60$, $p < 0.001$).

Chlorophyll-*a* concentrations were enhanced in the vertical profiles in the Oyashio region, where the concentrations of halocarbons such as CH_3Cl , CH_3Br , CH_2I_2 , and CH_2ClI were not enhanced. Other halocarbons (CH_3I , CH_2Br_2 , CH_2BrCl , CHBr_3 , CHBr_2Cl , and CHBrCl_2) showed no features in the vertical profiles and they are similar in concentration and/or in vertical pattern in the water column (0–100 m). These results suggest that the concentrations of halocarbons are not linked to bulk phytoplankton biomass in the present study. In the Atlantic Ocean, it has been reported that Chl.-*a* content does not necessarily correlate with the production of halogenated hydrocarbons (Schall *et al.* 1997). Abrahamsson *et al.* (2004a) also reported that no strong relationship was observed between the surface water concentrations of halocarbons and the total Chl.-*a* along a transect in the Southern Ocean. In *Phaeocystis* sp. (Prymnesiophyta) cultures, the CH_3Br concentration increased, not during the exponential phase, but during the stationary

phase. The concentrations of CH_3Br per Chl.-*a* in the middle of the exponential phase and the stationary phase (or decline phase) were 0.35 and 1.1 $\text{pmol } \mu\text{g}^{-1}$ of Chl.-*a*, respectively (Sæmundsdóttir and Matrai 1998). Thus, the production of halocarbons per Chl.-*a* is not constant even in a mono culture. These results indicate the difficulty of estimating global halocarbon production and the necessity to determine the essential factors that control halocarbon production.

(3) Size-fractionated chlorophyll-*a* and methyl halide concentrations

The concentration and relative abundance of size-fractionated Chl.-*a* at a 5-m depth shows that the Tsugaru warm current region was characterized as having pico-sized phytoplankton as the major type of plankton in this study. This result suggested that regions (and/or periods) mainly dominated by pico-sized phytoplankton, as found in the Tsugaru warm current region in the present study, may satisfy the appropriate conditions for a high occurrence of halocarbons. The rates of halocarbon production by phytoplankton of different sizes in surface seawater in the Southern Atlantic Ocean showed that the smallest-sized fractions (0.4–2 μm) were generally the most efficient producers of halocarbons, CH_2I_2 and CH_2BrCl , per Chl.-*a* (Abrahamsson *et al.* 2004b). Abrahamsson *et al.* (2004b) concluded that the major producers of brominated and chlorinated halocarbons were not microphytoplankton, but nano- and pico-sized phytoplankton. These results, including those from our study, point to the importance of nano- and/or picoplankton as one of the main sources of halocarbons. In the Oyashio region, a high concentration of Chl.-*a* due to a diatom bloom was observed. Although the abundance of pico-sized phytoplankton in the Oyashio region was similar to the abundance of pico-sized phytoplankton in the Tsugaru warm cur-

rent region, the concentrations of halocarbons in the Oyashio region were not significantly different from those at the other sampling stations. These results suggest that halocarbons, such as CH_3Cl , CH_3Br , CH_2ClI , and CH_2I_2 , were probably not produced by the diatom-dominated bloom at this site and production of these compounds could be affected by species of pico-sized phytoplankton and/or the composition of the assemblage of microorganisms. Hughes *et al.* (2008) reported that volatile iodocarbons were produced from biogenic marine aggregates. Marine aggregates exhibit diversity in organic matter content and microbial composition between different geographic locations and depths in the water column, and this variability could affect the iodocarbon production rate (Hughes *et al.* 2008). This result also suggests that the composition of microorganisms leads to variations in halocarbon productions.

(4) Phytoplankton pigments and methyl halide concentrations

High concentrations of chlorophyll-*b* (Chl.-*b*) and prasinoxanthin were observed in the Tsugaru warm current region where high CH_2I_2 concentration was observed, and these two pigments had a statistically significant positive correlation with CH_2I_2 ($r^2 = 0.69$ ($n = 7$, $p < 0.1$) and $r^2 = 0.71$ ($n = 7$, $p < 0.1$), respectively) and with CH_2ClI ($r^2 = 0.87$ ($n = 7$, $p < 0.01$) and $r^2 = 0.77$ ($n = 7$, $p < 0.01$), respectively), whereas high concentrations of CH_2I_2 and Chl.-*a* were not observed at the same sampling station (Fig. 8). Chlorophyll-*b* and prasinoxanthin are contained in some species of prasinophytes that belong to the Type 3 pigment group (Egeland *et al.* 1997; Jeffrey and Wright 2006). No laboratory culture experiment suggests the production of CH_2I_2 or CH_2ClI by prasinophytes to date. However, our results indicate that some species of prasinophytes might contribute to CH_2I_2 and CH_2ClI production.

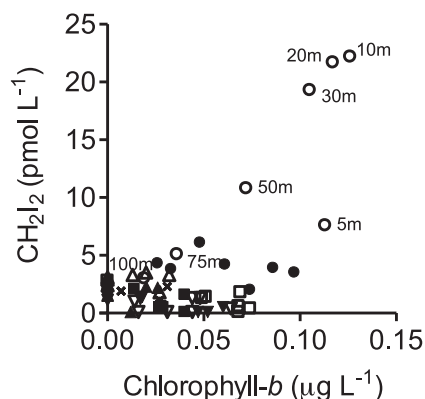


Fig. 8. Correlation between CH_2I_2 and chlorophyll-*b* concentrations in the surface seawater (modified from Kurihara *et al.* (2010)).

Additionally, it is known that numerous species of prasinophytes are pico-sized phytoplankton (Guillou *et al.* 2004). This does not conflict with our speculation that the existence of pico-sized phytoplankton might affect the production of halomethanes.

(5) Seawater concentrations, air mixing ratios, and sea-to-air fluxes of methyl halides

The average (range) mixing ratios of CH_2ClI were 0.27 (0.03–0.90) pptv in the western North Pacific (present study), 0.32 (0.18–0.71) pptv in the Atlantic and Southern Oceans (Chuck *et al.* 2005), and 0.15 (0.01–1.6) pptv in the North Atlantic (Varner *et al.* 2008). Our results were not higher than these previous data. In the Tsugaru warm current region (Stn. D2), where the CH_2ClI concentration in surface seawater reached 5.4 pmol L^{-1} , the mixing ratio of CH_2ClI in the air was 0.57 pptv (Fig. 9). In the open ocean, the input of iodine into the marine boundary layer is dominated by volatile iodinated organic compounds (reviewed in Carpenter (2003)). It was suggested that CH_2I_2 and CH_2ClI are potentially more significant

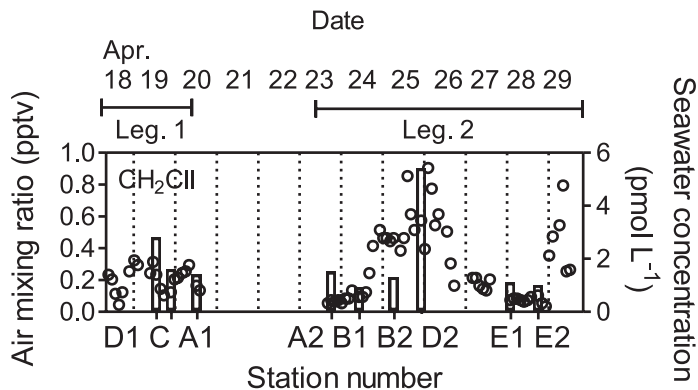


Fig. 9. CH_2ClI in the surface seawater and atmosphere. Bars and open circles indicate seawater concentrations and air mixing ratios, respectively (modified from Kurihara *et al.* (2010)).

sources of reactive iodine in the marine boundary layer than CH_3I , because of their shorter photolytic lifetimes (Chuck *et al.* 2005), and halogens have a substantial impact on regional, and possibly even global, ozone levels (von Glasow 2008; Read *et al.* 2008). Thus, the production and decomposition of CH_2I_2 and CH_2ClI in the ocean may affect the iodine budget in the atmosphere. There was a good correlation between Chl.-*a* concentration and isoprene concentration in our study. On the other hand, the Chl.-*a* concentration was not correlated with the concentrations of CH_3Br , CH_2I_2 and CH_2ClI in seawater. The highest concentrations of CH_3Br , CH_2ClI , and CH_2I_2 were observed at the sampling stations where pico-sized phytoplankton dominated (in the Tsugaru warm current region), and the concentrations of Chl.-*b* and prasinoxanthin had a statistically significant positive correlation with the concentration of CH_2I_2 or CH_2ClI (Stn. D2). These results indicate that picoplankton might be an important source of halocarbons, and that some species of prasinophytes might contribute to the production of CH_2I_2 and CH_2ClI . In future studies, the relationships between iodocarbon production and the characteristics of microorganisms, such as species

composition, size, and bacterial activity, should be taken into consideration in order to evaluate the importance of biogenic iodocarbon emissions from the open ocean.

4. Elucidation of the mechanism of methyl halide emission from marine phytoplankton: enzymatic and genetic analyses of key enzymes catalyzing the formation of CH_3I

To examine the relationships between HTMT activity and the emission strength of methyl halides, several marine phytoplankton that are reported to have HTMT activity (Itoh *et al.* 2009), marine diatoms and marine picoplankton, including *Ostreococcus* sp. and *Synechococcus* sp. were cultured. After cultivation, phytoplankton were collected by centrifugation and incubated with sea water containing 5 mM potassium iodide in a headspace vial, and the quantity of CH_3I and the HTMT activity of crude cell extracts were assayed by GC-MS (Table 4). From the results, it became clear that various phytoplankton including *Pavlova* sp., a marine diatom *Phaeodactylum tricorutum*, as well as the picoplankton *Ostreococcus* sp. and *Synechococcus* sp., emit CH_3I . In this study, we first observed that *P. tricorutum* CCAP1055/1,

Table 4. HTMT activity and rate of CH₃I emission from various marine phytoplankton.

Strain	HTMT activity (pmol/min/g cell)	CH ₃ I productivity (pmol/g cell/day)
<i>Phaeodactylum tricornutum</i> CCAP1055/1	27.9	2431.9
<i>Pavlova pinguis</i> CCAP940/2	100.6	603.6
<i>Pavlova pinguis</i> NBRC102807	0.6	428.3
<i>Pavlova gyrans</i> CCAP940/1B	62.9	537.7
<i>Isochrysis galbana</i> NBRC102813	30.4	0.0
<i>Nannochloris atomus</i> CCAP251/4A	1.0	0.0
<i>Ostreococcus</i> sp. CCMP2972	<0.1	391.5
<i>Thalassiosira pseudonana</i> CCMP1335	<0.1	64.0
<i>Nannochloropsis salina</i> CCMP1776	<0.1	668.1
<i>Agmenellum quadruplicatum</i> CCAP1400/1 (<i>Synechococcus</i> sp.)	<0.1	296.3

Ostreococcus sp. CCMP2972, and *Synechococcus* sp. CCAP1400/1 have HTMT activity and emit CH₃I. The marine diatom *P. tricornutum* showed the highest rate of CH₃I emission (2,432 pmol/g cell/day) among the tested specimens, although its HTMT activity was weaker than that of other microalgae such as *P. pinguis* CCAP 940/2 and *P. gyrans* CCAP 940/1, which showed lower rates of CH₃I emission (538–604 pmol/g cell/day). Considering the HTMT activity in the assessed phytoplankton and the CH₃I generation rates (Table 4), its HTMT activity did not linearly correlate with the amount of CH₃I emitted, although the HTMT activity was indispensable for producing CH₃X. Itoh *et al.* (1997) reported that *P. gyrans* CS-213 produces a large amount of methyl halides while *N. atomus* emits only trace amounts. Thus, the emission level of CH₃I corresponds with HTMT activity in crude cell extracts. In this study, however, we observed apparent exceptions between the CH₃I emission level and HTMT activity in crude cell extracts. Such a discrepancy might be caused by factors related to differences in enzymatic properties between the variants of HTMT, such as K_m values for I⁻, or concentration and form of iodide ions (I⁻, IO₃⁻, or I₂) in algal cells, since the concentration of free I⁻ in sea water is relatively low (0.012 ppm). The concentration of iodine in oceanic water is around

0.041 ppm when including iodic acid (IO₃⁻: 0.029 ppm) and iodide ions. This fact strongly suggests that the intracellular concentration of iodide ion (I⁻) is an important factor for producing CH₃I by HTM/HTMT reaction, and thus a specific system for regulating the concentration of I⁻ likely exists.

The mechanism regulating I⁻ concentration in algal cells via haloperoxidase (Kamenarska *et al.* 2007) is advocated in the marine macroalgae *Laminaria digitata* (Leblanc *et al.* 2006) and in various marine flavobacteria (Amachi *et al.* 2007) as follows: I⁻ is oxidized to HIO by haloperoxidase located in the cell wall; then, HIO and free I⁻ spontaneously form iodine. The hydrophobic property of iodine enables it to pass through the cell membrane. The existence of such an accumulation mechanism is speculated in marine phytoplankton, because the amount of CH₃I notably increased when the concentration of I⁻ was increased in sea water for incubation. However, the concentration mechanism of I⁻ in marine phytoplankton is still unknown. On the other hand, in this study we have confirmed that about 10% of the generated CH₃I was converted into CH₃Cl by the chemical reaction of Cl⁻ in the sea water. The mechanism of methyl halide generation in marine phytoplankton is illustrated in Fig. 10 (Toda and Itoh 2010).

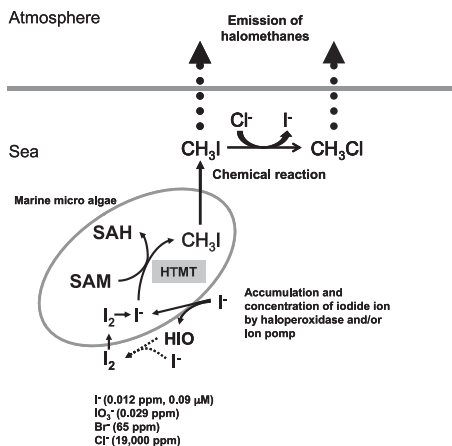


Fig. 10. Schematic model of methyl halide biosynthesis in marine phytoplankton.

HTMT genes were cloned from *P. tricornerutum* CCAP1055/1, *Ostreococcus* sp. CCMP2972, and *Synechococcus* sp. (*Agmenellum*) CCAP1400/1, and the HTMT gene of *P. tricornerutum* was expressed in *E. coli* and characterized in detail to clarify the HTMT reaction at the molecular level. The *P. tricornerutum* HTMT (PtHTMT) gene was isolated by in silico screening on the *P. tricornerutum* genome database on the basis of the HTMT gene (RsHTMT) of *Raphanus sativus* (daikon radish) (Itoh *et al.* 2009). We detected one homologous gene in the *P. tricornerutum* genome database (Scala *et al.* 2002) indicating an homology of about 30% with RsHTMT. PtHTMT was cloned and successfully expressed in *E. coli* with the aid of chaperones, and the gene was characterized in detail (Toda and Itoh 2010).

Recombinant PtHTMT was obtained as a soluble protein with a histidine tag at the C-terminus and successfully purified by Ni-Sepharose resin column chromatography. The molecular weight of the recombinant PtHTMT, estimated from HPLC analysis, was 30 kDa, suggesting that the native enzyme is a monomer. Substrate specificity and enzymatic prop-

erties of recombinant PtHTMT were characterized. As shown in Table 4, the K_m values for each substrate of recombinant PtHTMT revealed a similar trend to those of previously reported HTMTs and exhibited high specificity for I⁻, [SH]⁻, and [SCN]⁻, and low specificity for Cl⁻ and Br⁻. No HTMT activity toward IO₃⁻ was observed. Recombinant PtHTMT exhibited similar specificities for these substrates, except that the specificity for [SCN]⁻ was much lower than that for RsHTMT (Table 5). Considering the K_m and k_{cat}/K_m values of PtHTMT, it was concluded that the enzyme is specific to I⁻ and is adapted to the production of CH₃I.

We also succeeded in cloning the HTMTs from *Ostreococcus* sp. CCMP2972 and *Synechococcus* sp. (*Agmenellum quadruplecatum*) CCAP 1400/1, which are picoplankton (i.e., cyanobacteria and pico-eukaryotes) characterized by a cell size of 0.2–2 μm. *Ostreococcus* sp. is widely distributed in various marine environments and inhabits the lower layer of the euphotic zone in the ocean. *Synechococcus* sp. distribution ranges from the coastal euphotic zone to the pelagic euphotic zone (except in the polar regions), and is particularly dominant in areas of upwelling and in coastal regions containing moderate nutrition. At least we could detect the activity of recombinant *Ostreococcus* HTMT expressed in *E. coli*. The detailed characterizations of these recombinant HTMTs are under investigation. However, we were not able to cultivate *Prochlorococcus* sp., which is known to be dominant over *Synechococcus* sp. in oceans with poor nutrition. The phylogenetic tree of PtHTMT-homologous proteins is shown in Fig. 11. Interestingly, PtHTMT exhibits a greater similarity to HMT/HTMTs of higher plants than to those of unicellular algae such as *Ostreococcus tauri*. The present analysis also indicates that the homology of HTMTs across marine phytoplankton is low.

Table 5. Kinetic parameters of PtHTMT and RsHTMT.

	<i>P. tricornutum</i> HTMT		<i>R. sativus</i> HTMT	
	K_m (mM)	V_{max} (pmol/min/mg)	K_m (mM)	V_{max} (pmol/min/mg)
SAM	0.02	15235	0.19	—
Cl ⁻	637.9	625 (0.6%)	1657.4	3381 (2.4%)
Br ⁻	72.8	2096 (2.0%)	177.3	34965 (25%)
I ⁻	8.6	104266 (100%)	4.5	139286 (100%)
[SH] ⁻	9.9	76923 (73.8%)	12.2	158732 (114%)
[SCN] ⁻	7.9	20612 (19.8%)	0.04	185185 (133%)
IO ₃ ⁻	ND	ND	—	—

ND: not detected.

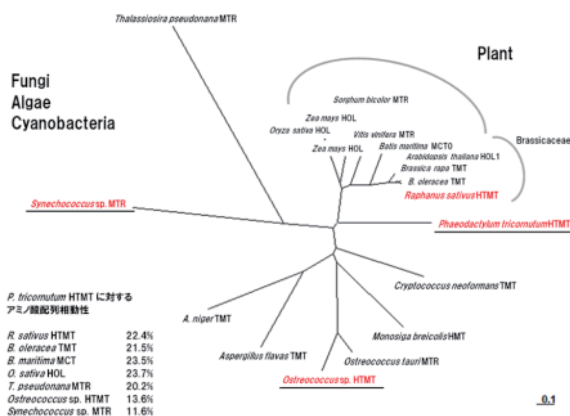


Fig. 11. Phylogenetic tree of PtHTMT homologous proteins.

Conclusions

In this study, we have improved our understanding of the production and emission of marine-derived volatile halocarbons. Major conclusions are as follows:

(1) We investigated the seasonal variation in atmospheric CH₃I at high-, mid-, and low-latitude sites in both hemispheres. In marine boundary air at mid-latitudes, the CH₃I concentration was well correlated with SST. This finding is consistent with previous observation, supporting the conclusion therein that CH₃I could be produced photochemically from organic com-

pounds in the surface seawater. The positive correlation between CH₃I fluxes and SST suggests that a future SST change might create an imbalance of iodine chemistry in the atmosphere. The highest median mixing ratio of CH₃I was observed over San Cristobal Island, which is on the equator in the eastern Pacific, suggesting that high bioproductivity is also likely to be an important factor controlling CH₃I emission. In the Arctic and in Antarctica, the lowest concentrations of CH₃I were found.

We have also obtained the first precise, full-year data sets of four iodocarbons in the atmosphere at two remote marine sites,

Hateruma Island and Cape Ochiishi, providing new insight into their possible sources and sinks. Diurnal variation of CH_2ClI and CH_2I_2 was very prominent, and the highly photolabile CH_2I_2 was rarely observed in the atmosphere at mid-day. Nighttime atmospheric CH_2ClI was strongly correlated with wind speed at Hateruma Island in the subtropical ocean, suggesting the ubiquitous presence of CH_2ClI at a fairly constant concentration. Using box model calculations, we roughly estimated the hourly sea-to-air flux of CH_2ClI to be a few tens of nanograms per square meter. CH_3I and $\text{C}_2\text{H}_5\text{I}$ showed very similar variations at both sites, suggesting common sources and sinks.

(2) We conducted halocarbon monitoring in air and surface seawater from polar to tropical oceans, to understand the spatial distributions of oceanic halocarbons. The on-board online multi-component halocarbon monitoring system was employed for the W-PASS cruises. The partial pressures of halocarbons both in surface seawater and air were measured to calculate the saturation anomaly. We compared the saturation anomalies of oceanic halocarbons with those of anthropogenic inert gases such as CFC-11 and HCFC-22, to subtract the physical effect (i.e., air-sea exchange and water mixing) from the saturation anomaly change. Some important aspects of oceanic halocarbons were found, (1) in the subarctic water, CH_3Cl and CH_3Br in surface seawater were undersaturated with respect to the air, whereas the saturation anomaly of CH_3I was high; (2) in the subtropical water, CH_3Br in surface seawater was undersaturated, whereas, the saturation anomalies of CH_3Cl and CH_3I were considerably high; and (3) in the mixed water with high biological productivity, various oceanic halocarbons including 3 monohalomethanes were supersaturated. The saturation anomalies of oceanic halocarbons are controlled by their produc-

tion and decomposition balance in each water mass as well as the sea-air exchange and the water mixing. We presumed that production/decomposition processes are related to temperature dependent biological and/or chemical reactions. Further researches on the time-series halocarbon monitoring and verification experiments for studies of the process, are needed to predict the oceanic halocarbon flux change.

(3) The peaks of CH_3Br , CH_2ClI , and CH_2I_2 were observed in the region where concentrations of chlorophyll-*a* were not as high ($0.65 \mu\text{g L}^{-1}$). The results of chlorophyll-*a* size fractionation showed a high occurrence of halomethanes in the stations dominated by pico-sized phytoplankton. These results indicate the importance of picoplankton as a possible source of halocarbon production. Chlorophyll-*b* and prasinoxanthin had a statistically significant positive correlation with CH_2I_2 ($r^2 = 0.69$ and $r^2 = 0.71$, respectively) and with CH_2ClI ($r^2 = 0.87$ and $r^2 = 0.77$, respectively), whereas chlorophyll-*a* did not correlate with any halocarbons. These results suggest that some species of prasinophytes might contribute to CH_2I_2 and CH_2ClI production. For other compounds, there was no peak in the vertical profile in seawater. In the depth profiles, the peak of CH_2ClI was observed above the peak of CH_2I_2 ; these profiles suggest that a photochemical reaction could yield CH_2ClI from CH_2I_2 in seawater. The mean mixing ratio and range of CH_3Cl , CH_3Br , and CH_2ClI in the air were measured as 548 (524–609), 12.1 (8.6–19.0), and 0.27 (0.03–0.90) pptv, respectively. CH_2I_2 was not detected in the atmosphere (<1 pptv). The highest mixing ratio of CH_2ClI in air was also observed near the station at which the highest concentration of CH_2ClI was observed in seawater; the sea-to-air fluxes of CH_2ClI and CH_2I_2 were 3.8 and $1.6 \text{ nmol m}^{-2} \text{ day}^{-1}$, respectively. These results suggest that the production of CH_2ClI and CH_2I_2

in seawater is an important source of organic iodine compounds in the remote atmosphere.

(4) The following results clarified the biogenic emission of CH_3I in oceans: CH_3I is produced directly in phytoplankton and is catalyzed by an HTMT reaction; the produced CH_3I is partly converted into CH_3Cl in sea water; the amount of CH_3I emission

varies dramatically across plankton species; an unknown concentration mechanism of I^- is another key issue for estimating CH_3I emission from phytoplankton; HTMT enzymes in marine phytoplankton are diverse. Therefore, the amount of CH_3I from the marine environment cannot be easily estimated from the total biomass of phytoplankton in a given region.

References

- Abrahamsson K, Bertilsson S, Chierici M, Fransson A, Froneman PW, Lorén A, Pakhomov EA (2004a) Variations of biochemical parameters along a transect in the Southern Ocean, with special emphasis on volatile halogenated organic compounds. *Deep-Sea Res. II* **51**: 2745–2756.
- Abrahamsson K, Lorén A, Wulff A, Wängberg S-Å (2004b) Air-sea exchange of halocarbons: the influence of diurnal and regional variations and distribution of pigments. *Deep-Sea Res. II* **51**: 2789–2805.
- Amachi S, Kamagata Y, Kanagawa T, Muramatsu Y (2001) Bacteria mediate methylation of iodine in marine and terrestrial environments. *Appl. Environ. Microbiol.* **67**: 2718–2722.
- Amachi S, Kimura K, Muramatsu Y, Shinoyama H, Fujii T (2007) Hydrogen peroxide-dependent uptake of iodine by marine Flavobacteriaceae bacterium strain C-21. *Appl. Environ. Microbiol.* **73**: 7536–7541.
- Attieh J, Kleppinger-Sparace KF, Nunes *et al.* (2000) Evidence implicating a novel thiol methyltransferase in the detoxification of glucosinolate hydrolysis products in *Brassica oleracea* L. *Plant Cell Environ.* **23**: 165–174.
- Butler JH, King DB, Lobert JM, Montzka SA, Yvon-Lewis SA, Hall BD, Warwick NJ, Mondeel DJ, Aydin M, Elkins JW (2007) Oceanic distributions and emissions of short-lived halocarbons. *Global Biogeochem. Cycles* **21**: GB1023, doi:10.1029/2006GB002732.
- Carpenter LJ (2003) Iodine in the marine boundary layer. *Chem. Rev.* **103**: 4953–4962.
- Chuck AL, Turner SM, Liss PS (2005) Oceanic distributions and air-sea fluxes of biogenic halocarbons in the open ocean. *J. Geophys. Res.* **110**: C10022, doi:10.1029/2004JC002741.
- Egeland ES, Guillard RRL, Liaaen-Jensen S (1997) Additional carotenoid prototype representatives and a general chemosystematic evaluation of carotenoids in prasinophyceae (chlorophyta). *Phytochemistry* **44**: 1087–1097.
- Enomoto T, Yokouchi Y, Izumi K, Inagaki T (2005) Development of an analytical method for atmospheric halocarbons and its application to airborne observation. *J. Jpn. Soc. Atmos. Environ.* **40**(1): 1–8.
- Guillou L, Eikrem W, Chrétiennot-Dinet M-J, Le Gall F, Massana R, Romarid K, Pedrós-Alió C, Vault D (2004) Diversity of picoplanktonic prasinophytes assessed by direct nuclear SSU rDNA sequencing of environmental samples and novel isolates retrieved from oceanic and coastal marine ecosystems. *Protist* **155**: 193–214.
- Hanawa K, Mitsudera H (1987) Variation of water system distribution in the Sanriku Coastal Area. *J. Oceanogr. Soc. Jpn.* **42**: 435–446.
- Hughes C, Malin G, Turley CM, Keely BJ, Nightingale PD (2008) The production of volatile iodocarbons by biogenic marine aggregates. *Limnol. Oceanogr.* **53**: 867–872.
- Hunter-Smith RJ, Balls PW, Liss PS (1983) Henry's law constants and the air-sea exchange of various low molecular weight halocarbon gases. *Tellus* **35B**: 170–176.
- Itoh N, Tsujita M, Ando T, Hisatomi G, Higashi T (1997) Formation and emission of monohalomethanes from marine algae. *Phytochemistry* **45**: 3147–3153.
- Itoh N, Toda H, Matsuda M, Negishi T, Taniguchi T, Ohsawa N (2009) Involvement of S-adenosylmethionine-dependent halide/thiol methyltransferase (HTMT) in methyl halide emissions from agricultural plants: isolation and characterization of an HTMT-coding gene from *Raphanus sativus* (daikon radish). *BMC Plant Biol.* **9**: 116.

- Jeffrey SW, Wright SW (2006) Photosynthetic pigments in marine microalgae: Insights from cultures and the sea. p. 33–90. In *Algal Cultures, Analogues of Blooms and Applications* (ed. Rao DVS), Science Publishers, Enfield, NH, U.S.A.
- Kamenarska Z, Taniguchi T, Ohsawa N, Hiraoka M, Itoh N (2007) A vanadium-dependent bromoperoxidase in the marine red alga *Kappaphycus alvarezii* (Doty) Doty displays clear substrate specificity. *Phytochemistry* **68**: 1358–1366.
- King DB, Butler JH, Montzka SA, Yvon-Lewis SA, Elkins JW (2000) Implications of methyl bromide supersaturations in the temperate North Atlantic Ocean. *J. Geophys. Res.* **105**: 19763–19769.
- King DB, Butler JH, Yvon-Lewis SA, Cotton SA (2002) Predicting oceanic methyl bromide saturation from SST. *Geophys. Res. Lett.* **29**: 2199, doi:10.1029/2002GL016091.
- Kurihara MK, Kimura M, Iwamoto Y, Narita Y, Ooki A, Eum Y-J, Tsuda A, Suzuki K, Tani Y, Yokouchi Y, Uematsu M, Hashimoto S (2010) Distributions of short-lived iodocarbons and biogenic trace gases in the open ocean and atmosphere in the western North Pacific. *Mar. Chem.* **118**: 156–170.
- Leblanc C, Colin C, Cosse A, Delage L, La Barre S, Morin P, Fievet B, Voiseux C, Ambroise Y, Verhaeghe E, Amouroux D, Donard O, Tessier E, Potin P (2006) Iodine transfers in the coastal environment: the key role of brown algae and of their vanadium-dependent haloperoxidases. *Biochimie* **88**: 1773–1785.
- Li SM, Yokouchi Y, Barrie LA, Muthuramu K, Shepson PB, Bottenheim JW, Sturges WT, Landsberger S (1994) Organic and inorganic bromine compounds and their composition in the Arctic troposphere during polar sunrise. *J. Geophys. Res.* **99**(D12): 25415–25428.
- Moore RM (2000) The solubility of a suite of low molecular weight organochlorine compounds in seawater and implications for estimating the marine source of methyl chloride to the atmosphere. *Chemosphere* **2**: 95–99.
- Moore RM, Tokarczyk R (1993) Volatile biogenic halocarbons in the northwest Atlantic. *Global Biogeochem. Cycles* **7**: 195–210.
- Moore RM, Geen CE, Tait VK (1995) Determination of Henry's law constants for a suite of naturally occurring halogenated methanes in seawater. *Chemosphere* **30**: 1183–1191.
- Moore RM, Groszko W, Niven SJ (1996) Ocean-atmosphere exchange of methyl chloride: Results from NW Atlantic and Pacific Ocean studies. *J. Geophys. Res.* **101**: 28529–28538.
- Mössinger JC, Shallcross DE, Cox RA (1998) UV-VIS absorption cross-sections and atmospheric lifetimes of CH_2Br_2 , CH_2I_2 and CH_2BrI . *J. Chem. Soc., Faraday Trans.* **94**(10): 1391–1396.
- Ooki A, Yokouchi Y (2008) Development of a silicone membrane tube equilibrator for measuring partial pressures of volatile organic compounds in natural water. *Environ. Sci. Technol.* **42**: 5706–5711.
- Ooki A, Yokouchi Y (2011a) Dichloromethane in the Indian Ocean: Evidence for in-situ production in seawater. *Mar. Chem.* **124**: 119–124.
- Ooki A, Yokouchi Y (2011b) Determination of Henry's law constant of halocarbons in seawater and analysis of sea-to-air flux of iodoethane ($\text{C}_2\text{H}_5\text{I}$) in the Indian and Southern oceans based on partial pressure measurements. *Geochem. J.* **45**: e1–e7.
- Ooki A, Tsuda A, Kameyama S, Takeda S, Itoh S, Suga T, Tazoe H, Okubo A, Yokouchi Y (2010) Methyl halides in surface seawater and marine boundary layer of the Northwest Pacific. *J. Geophys. Res.* **115**: C10013, doi:10.1029/2009JC005703.
- Rattigan OV, Barrett E, Clark M (1997) UV absorption cross-sections and atmospheric photolysis rates of CF_3I , CH_3I , $\text{C}_2\text{H}_5\text{I}$ and CH_2ICl . *J. Chem. Soc., Faraday Trans.* **93**: 2839–2846.
- Read KA, Mahajan AS, Carpenter LJ, Evans MJ, Faria BVE, Heard DE, Hopkins JR, Lee JD, Moller SJ, Lewis AC, Mendes L, McQuaid JB, Oetjen H, Saiz-Lopez A, Pilling MJ, Plane JMC (2008) Extensive halogen-mediated ozone destruction over the tropical Atlantic Ocean. *Nature* **453**: 1232–1235.
- Richter U, Wallace DWR (2004) Production of methyl iodide in the tropical Atlantic Ocean. *Geophys. Res. Lett.* **31**(23): L23S03, doi:10.1029/2004GL020779.
- Sander R (1999) Compilation of Henry's Law Constants for Inorganic and Organic Species of Potential Importance in Environmental Chemistry (Version 3). <http://www.henrys-law.org>
- Scala S, Carels N, Falciatore A, Chiusano ML, Bowler C (2002) Genome properties of the diatom *Phaeodactylum tricorutum*. *Plant Phys.* **129**: 993–1002.
- Schall C, Heumann KG, Kirst GO (1997) Biogenic volatile organoiodine and organobromine hydrocarbons in the Atlantic Ocean from 42°N to 72°S. *Fresenius' J. Anal. Chem.* **359**: 298–305.
- Simmonds PG, Manning AJ, Cunnold DM, McCulloch A, O'Doherty S, Derwent RG, Krummel PB, Fraser PJ, Dunse B, Porter LW, Wang RHJ, Grealley BR, Miller BR, Salameh P, Weiss RF, Prinn RG (2006) Global trends, seasonal cycles, and European emissions of dichloromethane, trichloroethene,

- and tetrachloroethene from the AGAGE observations at Mace Head, Ireland, and Cape Grim, Tasmania. *J. Geophys. Res.* **111**: D18304, doi:10.1029/2006JD007082.
- Sæmundsdóttir S, Matrai PA (1998) Biological production of methyl bromide by cultures of marine phytoplankton. *Limnol. Oceanogr.* **43**: 81–87.
- Toda H, Itoh N (2010) Isolation and characterization of gene encoding S-adenosyl-L-methionine-dependent halide/thiol methyltransferase (HTMT) from marine diatom *Phaeodactylum tricornutum*: Biogenic mechanism of CH₃I emissions in oceans. *Phytochemistry* **72**: 337–343.
- Varner RK, Zhou Y, Russo RS, Wingenter OW, Atlas E, Stroud C, Mao H, Talbot R, Sive BC (2008) Controls on atmospheric chloriodomethane (CH₂ClI) in marine environments. *J. Geophys. Res.* **113**: D10303, doi:10.1029/2007JD008889.
- von Glasow R (2008) Atmospheric chemistry: Sun, sea and ozone destruction. *Nature* **453**: 1195–1196.
- Wanninkhof R (1992) Relationship between wind-speed and gas-exchange over the ocean. *J. Geophys. Res.-Oceans* **97**(C5): 7373–7382.
- Wilhelm E, Battino R, Wilcock RJ (1977) Low-pressure solubility of gases in liquid water. *Chem. Rev.* **77**: 219–262.
- Wuosmaa AM, Hager LP (1990) Methyl chloride transferase: a carbocation route for biosynthesis of halometabolites. *Science* **249**: 160–162.
- Yamamoto H, Yokouchi Y, Otsuki A, Itoh H (2001) Depth profiles of volatile halogenated hydrocarbons in seawater in the Bay of Bengal. *Chemosphere* **45**: 371–377.
- Yokouchi Y, Mukai H, Yamamoto H, Otsuki A, Saitoh C, Nojiri Y (1997) Distribution of methyl iodide, ethyl iodide, bromoform, and dibromomethane over the ocean (east and southeast Asian seas and the western Pacific). *J. Geophys. Res.* **102**(D7): 8805–8809.
- Yokouchi Y, Nojiri Y, Barrie LA, Toom-Sauntry D, Fujinuma Y (2001) Atmospheric methyl iodide: High correlation with surface seawater temperature and its implications on the sea-to-air flux. *J. Geophys. Res.* **106**(D12): 12661–12668, doi:10.1029/2001JD900083.
- Yokouchi Y, Taguchi S, Saito T, Tohjima Y, Tanimoto H, Mukai H (2006) High frequency measurements of HFCs at a remote site in east Asia and their implications for Chinese emissions. *Geophys. Res. Lett.* **33**: L21814 doi:10.1029/2006GL026403.
- Yokouchi Y, Osada K, Wada M, Hasebe F, Agama M, Murakami R, Mukai H, Nojiri Y, Inuzuka Y, Toom-Sauntry D, Fraser P (2008) Global distribution and seasonal concentration change of methyl iodide in the atmosphere. *J. Geophys. Res.-Atmospheres* **113**(D18).
- Yokouchi Y, Saito T, Ooki A, Mukai H (2011) Diurnal and Seasonal Variations of Iodocarbons (CH₂ClI, CH₂I₂, CH₃I, and C₂H₅I) in the Marine Atmosphere. *J. Geophys. Res.-Atmospheres* **116**.
- Zafiriou OC (1975) Reaction of methyl halides with seawater and marine aerosols. *J. Marine Research* **33**: 75–81.
- Zheng DQ, Guo TM, Knapp H (1997) Experimental and modeling studies on the solubility of CO₂, CHClF₂, CHF₃, C₂H₂F₄ and C₂H₄F₂ in water and aqueous NaCl solutions under low pressures. *Fluid Phase Equilib.* **129**: 197–209.